Earth and Planetary Science Letters 298 (2010) 199–204

Contents lists available at ScienceDirect

Earth and Planetary Science Letters

journal homepage: www.elsevier.com/locate/epsl

Low silica activity for hydrogen generation during serpentinization: An example of natural serpentinites in the Mineoka ophiolite complex, central Japan

Ikuo Katayama *, Iori Kurosaki [1], Ken-ichi Hirauchi

Department of Earth and Planetary Systems Science, Hiroshima University, Higashi-Hiroshima 739-8526, Japan

ARTICLE INFO

Article history:
Received 30 April 2010
Received in revised form 26 July 2010
Accepted 29 July 2010
Available online 25 August 2010

Edited by: R.W. Carlson

Keywords:
serpentinite
magnetite
hydrogen
silica activity
hydrothermal vent system
microbial community

ABSTRACT

The textural evolution in the serpentinite of the Mineoka ophiolite complex has been investigated to constrain the natural environment for hydrogen production in the serpentinite-hosted hydrothermal vent systems. Textural relations of the serpentinites from the Mineoka ophiolite indicate at least two stages in the process of serpentinization, with the replacement of olivine by a mesh texture of serpentine and brucite, followed by the development of magnetite-bearing or -free serpentine veins. The generation of hydrogen during serpentinization, which accompanies the formation of magnetite, involves a silica-depletion reaction, as evidenced by the low abundance of serpentine in the magnetite-bearing veins and the absence of magnetite in pseudomorphs of orthopyroxene. Direct evidence for the production of hydrogen and strongly reducing conditions is provided by CH_4 and H_2-bearing inclusions in relic olivine crystals; the production of methane and hydrogen may have provided a suitable environment for microbial activity in hydrothermal vent systems along the seafloor. Our results indicate that low silica activity plays a key role in the generation of hydrogen during serpentinization, and that low silica activity environments are possible in olivine-rich rocks such as dunite, or during local disequilibrium in other silica-poor rocks in the mantle lithosphere.

1. Introduction

Microbial communities are known to exist in the vicinity of the seafloor where they take part in various chemical reactions (e.g., Corliss et al., 1979; Spiess et al., 1980; Baross and Hoffman, 1985; Takai et al., 2004). Remarkable submarine ecosystems have been reported in the serpentinite-hosted hydrothermal fields where hydrogen is a key product for the microbial activity (e.g., Holm and Charlou, 2001; Kelley et al., 2001, 2005; Nakamura et al., 2009). Serpentinites are formed by reaction between hydrothermal fluids and mantle rocks, and hydrogen and methane are released in the extremely reducing conditions. It is now generally thought that hydrothermal vents associated with serpentinized rocks played a key role in the genesis of life in the early oceans (e.g., Sleep et al., 2004; Martin et al., 2008), sparking renewed interest in water–rock interactions in the vicinity of the seafloor. It is important, therefore, to study the process of serpentinization, which is currently not well constrained in natural rock samples.

Under strongly reducing conditions, the formation of magnetite always generates hydrogen during serpentinization, following reactions such as:

$$3Fe_2SiO_4 + 2H_2O = 2Fe_3O_4 + 3SiO_2 + 2H_2$$

$$\text{olivine} + \text{water} = \text{magnetite} + \text{silica} + \text{hydrogen}. \quad (1)$$

Based on mineralogical and textural observations, a two stage model for serpentinization has been proposed, involving the early formation of brucite and serpentine followed by magnetite formation (e.g., Toft et al., 1990; Oufi et al., 2002; Bach et al., 2006; Beard et al., 2009). The first reaction is:

$$2(Mg,Fe)_2SiO_4 + 3H_2O = (Mg,Fe)_3Si_2O_5(OH)_4 + (Mg,Fe)(OH)_2$$

$$\text{olivine} + \text{water} = \text{serpentine} + \text{brucite}. \quad (2)$$

The products of this reaction often form a mesh texture after olivine.

For the second stage of the process of serpentinization, a number of reactions have been suggested, depending on the degree of silica activity. For example, Bach et al. (2006) proposed that the formation of magnetite, during the breakdown of ferroan brucite, is facilitated by relatively high silica activity, as follows:

$$9Fe(OH)_2 + 4SiO_2 = 2Fe_3Si_2O_5(OH)_4 + Fe_3O_4 + 4H_2O + H_2$$

$$\text{brucite} + \text{silica} = \text{serpentine} + \text{magnetite} + \text{water} + \text{hydrogen}. \quad (3)$$

* Corresponding author. Tel.: +81 824 24 7468; fax: +81 824 24 0735.
E-mail address: katayama@hiroshima-u.ac.jp (I. Katayama).
[1] Now at: Graduate School of Social and Cultural Studies, Kyushu University, Fukuoka 812-8581, Japan.

0012-821X/$ – see front matter © 2010 Elsevier B.V. All rights reserved.
doi:10.1016/j.epsl.2010.07.045

In contrast, Frost and Beard (2007) reported that the second stage of serpentinization reflects the inherent instability of ferroan serpentine during low silica activity, with the breakdown of the ferrous component to form magnetite, as follows:

$$Fe_3Si_2O_5(OH)_4 = Fe_3O_4 + 2SiO_2 + H_2O + H_2$$

$$\text{serpentine} = \text{magnetite} + \text{silica} + \text{water} + \text{hydrogen}. \quad (4)$$

Thus, the conditions for magnetite formation during serpentinization remain unclear, even though the process plays a key role in microbial activity in the extremely reducing conditions of the seafloor.

In this study, we described the mineralogical evolution of serpentinized peridotites from the Mineoka ophiolite complex, central Japan, discuss the processes of hydrogen generation during serpentinization, and comment on the environments which hosted microbial activity in these extreme conditions on Earth.

2. Sample description and petrography

Serpentinites were collected from the Mineoka belt, central Japan. This belt is recognized as an accreted ophiolite fragment with a mid-oceanic ridge affinity (e.g., Ogawa and Taniguchi, 1988; Sato et al., 1999). Peridotites in the Mineoka belt are mostly serpentinized as a result of extensive hydrothermal activity, and they are generally massive except near basaltic blocks. These ultramafic rocks contain relict minerals, including olivine (Fo_{90-93}), orthopyroxene (En_{89-91}), and Cr-rich spinel. Chemical compositions, and the lack of cumulate textures, suggest that the rocks originated as a residue from partial melting (Sato and Ogawa, 2000).

The massive serpentinites are characterized by mesh textures, which are pseudomorph after olivine. Orthopyroxene pseudomorphs made of bastite are also locally observed. Serpentine minerals in these pseudomorphs are lizardite and/or chrysotile, as identified by laser Raman spectroscopy and TEM observations (Hirauchi et al., 2010). The occurrence of low-temperature serpentines is a common feature of serpentinized peridotites on the seafloor (e.g., Wicks and Whittaker, 1977). Most serpentinites contain magnetite as either stringers or patches in late-stage veins that crosscut the mesh texture after olivine, but these veins do not directly contact with relict olivine crystals (Fig. 1A, B). Orthopyroxene is commonly replaced by serpentine (bastite), but magnetite is never observed in the serpentine-filled veins within orthopyroxene pseudomorphs (Fig. 1C, D). Chemical mapping shows the existence of several domains within the serpentine-filled veins that cut the replaced olivine. The domains are disposed as bands symmetrically about the center of the vein (Fig. 2). Most magnetite occurs in the Fe-rich central domains, surrounded by relatively Si-rich and Fe-poor domains.

The veins are composed of multiple phases on the submicron scale, and electron microprobe analysis (with a focused 3 μm beam) was used to identify the chemical compositions of each domain. The compositions of the serpentine-filled veins cutting olivine and orthopyroxene are shown in Fig. 3 and Table 1. Microprobe analyses indicate that the veins in olivine are mixtures of serpentine and brucite; the compositions fall on a straight line that connects stoichiometric serpentine and brucite (Fig. 3A). Similar mixtures of brucite and serpentine have been documented from the IODP drilled troctolites (Beard et al., 2009) and the Oman ophiolite complex (Baronnet and Boudier, 2001). The domains outside the veins (domain 1) exhibits the typical mesh texture of replaced olivine, and it has a composition relatively rich in Fe and poor in Si, reflecting the high concentration of brucite near the olivine–mesh contact. The olivine pseudomorphs are cut by later stage veins (Fig. 1), which are also mixtures of brucite and serpentine with distinct ratios of these minerals (Table 1). The veins are composed of relatively Si-rich bands with high abundance of serpentine (domain 2), and magnetite-bearing Si-poor domains in center portion (domain 3). Based on simple two end-member calculations, serpentine abundance is 97–99% in the Si-rich domains and 84–90% in the Si-poor domains, respectively.

Laser Raman analysis reveals that serpentines in domain 1 and 3 are lizardite characterized by double bands at 3685 and 3705 cm^{-1}, whereas those in domain 2 are mainly composed of chrysotile at

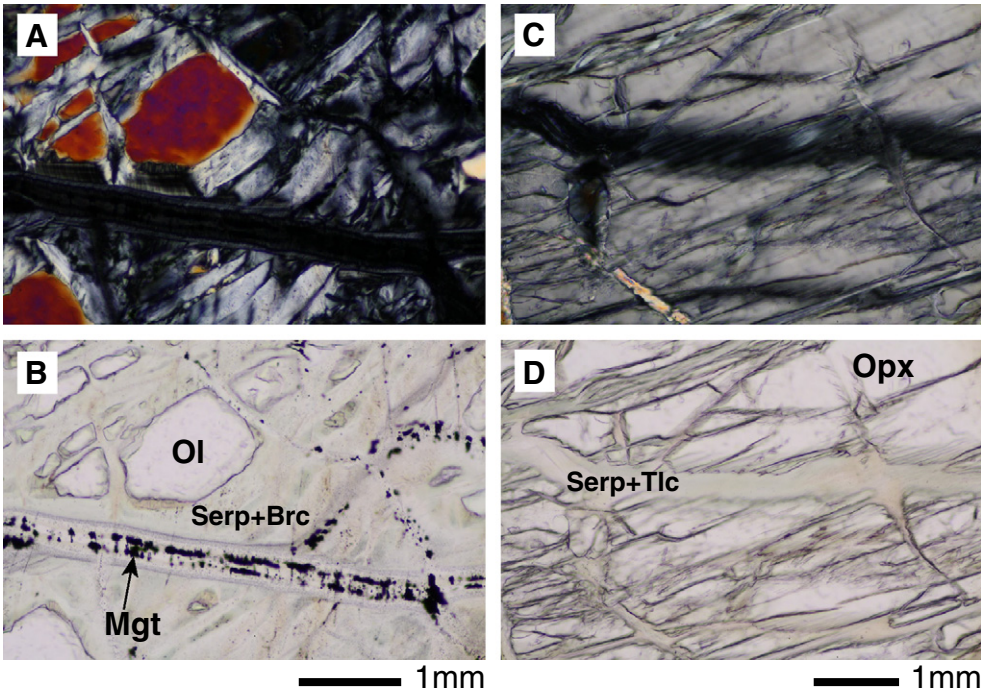

Fig. 1. Photomicrographs of serpentinized peridotites from the Mineoka ophiolite complex, showing serpentine after olivine (A: cross-polarized light, B: plane-polarized light) and after orthopyroxene (C: cross-polarized light, D: plane-polarized light). Magnetite occurs in the serpentine-filled veins that crosscut the mesh texture replacing olivine (A, B), whereas magnetite is absent in the serpentine-filled veins that crosscut orthopyroxene. Mineral abbreviations are, Ol: olivine, Mgt: magnetite, Serp: serpentine, Brc: brucite, Opx: orthopyroxene, and Tlc: talc.

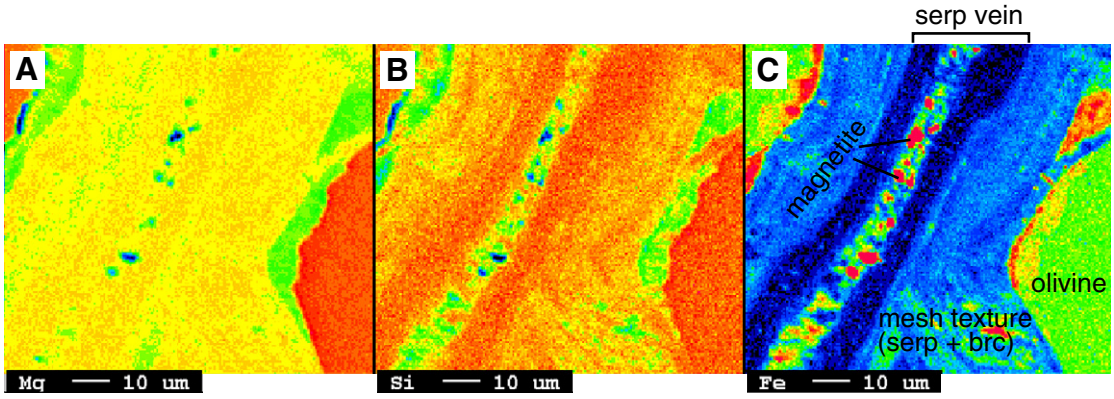

Fig. 2. Elemental mapping for Mg, Si, and Fe in serpentinized area near olivine. Colors correspond to the X-ray intensity, where bluish and reddish colors represent low and high intensities, respectively. The serpentinized areas are divided into three domains; the first is the mesh texture that replaces olivine (domain 1), the second is the magnetite-free material on either side of the central magnetite-bearing zone of serpentine veins (domain 2), and the third is the magnetite-bearing center of the serpentine veins (domain 3).

3701 cm^{-1} with additional bands of brucite (Fig. 4). Chrysotile is known to appear at isotropic stress environments of fluid-filled voids and pores, although it is highly unstable under stress associated with expansion, flattening and shear (Evans, 2004). Fe–Ni alloys, including awaruite ($FeNi_3$), are also identified in association with magnetite in the central domains (domain 3).

Serpentine-filled veins cutting orthopyroxene have a distinctive chemical composition, and in contrast to those cutting olivine, they do not contain different chemical domains. They have a substantially higher Al_2O_3 content (up to 2.9 wt.%) than those cutting olivine, and the sum of tetrahedral cations, silicon and aluminum, is significantly higher than in the serpentine end-member, indicating the presence of talc (Fig. 3B).

The Fe contents of these serpentine-filled veins are little scattered; X_{Fe} is ranging 0.04–0.12 after olivine, and X_{Fe} is 0.06–0.15 after orthopyroxene (Fig. 5). In the veins of olivine pseudomorph, the magnetite-free domain (domain 2) tends to show lower Fe contents compared to the other domains. Such variation may reflect the dominant serpentine phase, since the domain 2 is mainly composed of chrysotile whereas lizardite is a stable serpentine form in the domains 1 and 3 as identified by the Raman spectra. Similar trend of lower X_{Fe} in chrysotile has been also reported in the serpentinized olivine websterite from the Canyon Mountain complex (Evans et al., 2009).

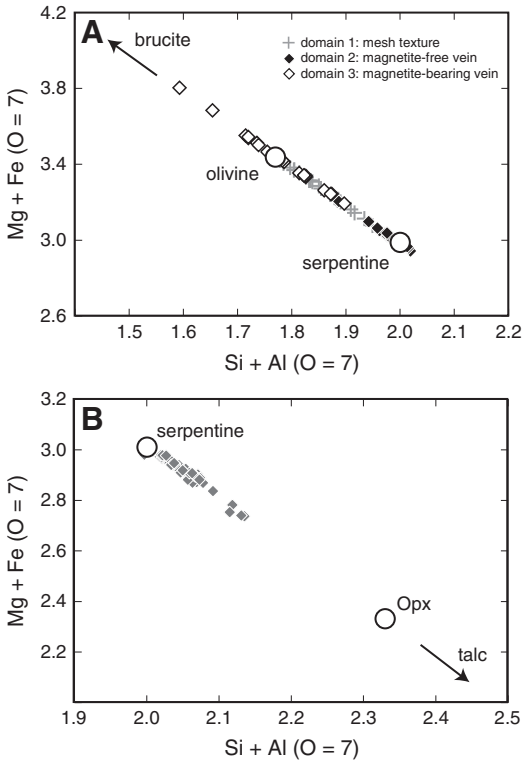

Fig. 3. Chemical composition of serpentine-filled veins after olivine (A) and orthopyroxene (B), as a function of Si + Al and Mg + Fe cations per 7 oxygens. The variations in chemical composition in domains of olivine replacement suggest mixtures of brucite and serpentine, whereas the composition where orthopyroxene has been replaced indicates a mixture of serpentine and talc. In serpentine-filled veins cutting olivine (A), the magnetite-bearing domains tend to have a higher brucite content than the magnetite-free domains.

Table 1
Chemical compositions of serpentines after olivine and orthopyroxene.

		Serpentines after olivine					
	Olivine	Domain 1	Domain 2	Domain 3	Opx	Serpentines after Opx	Serpentines after Opx
SiO_2	40.64	38.84	41.16	34.64	55.65	38.18	39.89
TiO_2	0.04	0.00	0.03	0.04	0.10	0.07	0.02
Al_2O_3	0.02	0.02	0.12	0.16	3.07	2.97	2.30
FeO*	8.50	5.35	3.20	7.15	5.54	6.01	6.28
MnO	0.16	0.07	0.03	0.08	0.17	0.23	0.18
Cr_2O_3	0.06	0.01	0.03	0.01	0.69	0.85	0.27
MgO	50.09	40.16	39.79	41.89	33.87	36.32	36.28
CaO	0.05	0.06	0.03	0.02	1.13	0.05	0.07
Na_2O	0.01	0.03	0.01	0.01	0.02	0.00	0.00
K_2O	0.00	0.00	0.03	0.01	0.00	0.00	0.00
NiO	0.41	0.30	0.07	0.00	0.14	0.11	0.04
Total	99.98	84.83	84.50	84.01	100.37	84.79	85.33
Cation per 7 oxygen atoms							
Si	1.738	1.909	1.991	1.755	2.235	1.879	1.942
Ti	0.001	0.000	0.001	0.002	0.003	0.003	0.001
Al	0.001	0.001	0.007	0.009	0.145	0.172	0.132
Fe	0.304	0.220	0.130	0.303	0.186	0.247	0.256
Mn	0.006	0.003	0.001	0.004	0.006	0.009	0.007
Cr	0.002	0.000	0.001	0.001	0.022	0.033	0.010
Mg	3.193	2.942	2.868	3.163	2.028	2.664	2.633
Ca	0.002	0.003	0.002	0.001	0.049	0.003	0.004
Na	0.001	0.002	0.001	0.001	0.001	0.000	0.000
K	0.000	0.000	0.002	0.000	0.000	0.000	0.000
Ni	0.012	0.010	0.002	0.000	0.004	0.004	0.001
Fe + Mg	3.50	3.16	3.00	3.47	2.21	2.91	2.89
X_{Fe}	0.09	0.07	0.04	0.09	0.08	0.08	0.09
Si + Al	1.74	1.91	2.00	1.76	2.38	2.05	2.07

*Total Fe calculated as FeO.

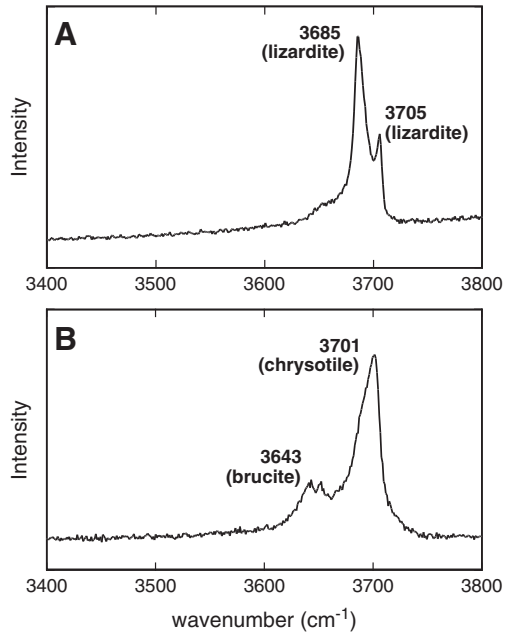

Fig. 4. Raman spectra of the serpentine-filled veins. (A) Mesh texture after olivine is represented by lizardite at double bands of 3685 and 3705 cm^{-1}, (B) magnetite-free veins after olivine are characterized by chrysotile at 3701 cm^{-1} as well as smaller bands of brucite at 3643 cm^{-1}.

3. Magnetite-forming reactions

Textural relationships clearly indicate at least two stages in the process of serpentinization in the Mineoka ophiolite complex, involving first the formation of a serpentine mesh texture after olivine, then magnetite-bearing serpentine-filled veins. The absence of magnetite in the mesh texture suggests reaction (2) as the first-stage process in the process of serpentinization of the Mineoka peridotites. The mesh texture is crosscut by magnetite-bearing veins, which are composed of two chemically distinct layers (Fig. 3A). Although two principle reactions of Eqs. (3) and (4) are possible, it is likely that reaction (4) was responsible for the formation of the magnetite, with magnetite in the Si-poor domains, representing the serpentine-out reaction. This reaction is also consistent with the low silica activity imposed by the brucite–serpentine assemblage (Fig. 6).

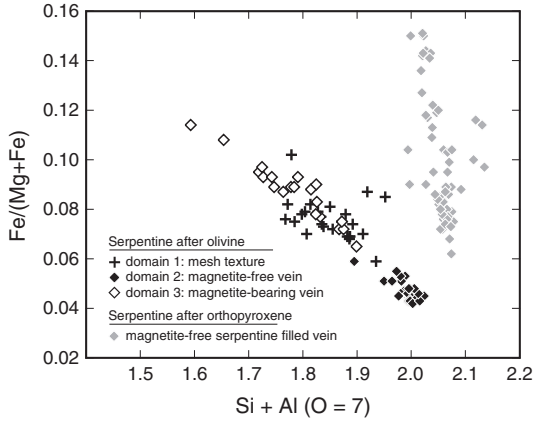

Fig. 5. Chemical composition of serpentine-filled veins after olivine and orthopyroxene, as a function of Fe value and Si + Al cations per 7 oxygens. The variation may reflect the stable serpentine phase (lizardite or chrysotile) in addition to the brucite abundance in the veins.

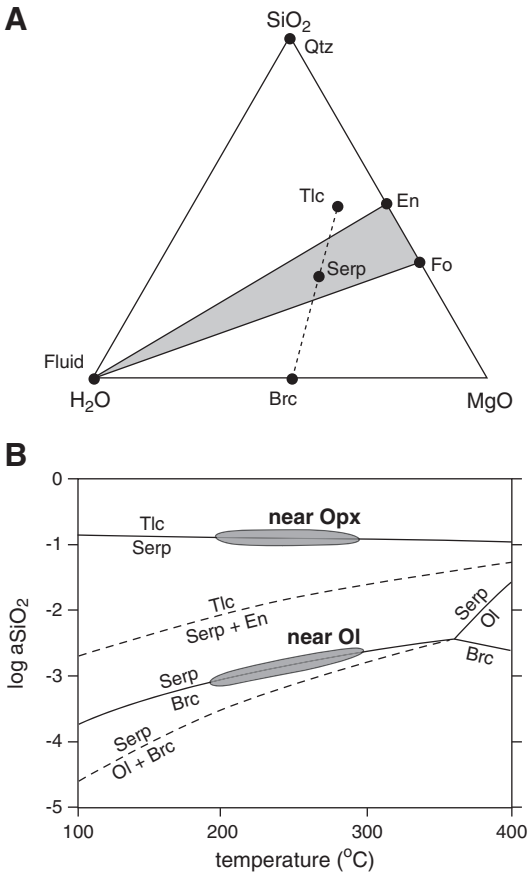

Fig. 6. (A) A phase composition in the $MgO–SiO_2–H_2O$ system and (B) silica activity in serpentinized areas calculated for a pressure of 1 kbar (Frost and Beard, 2008). The serpentine–talc assemblage after orthopyroxene indicates approximately two orders of magnitude higher silica activity than the serpentine–brucite assemblage after olivine. Quartz (Qtz), talc (Tlc), enstatite (En), forsterite (Fo), serpentine (Serp), brucite (Brc), olivine (Ol), orthopyroxene (Opx).

Although the Fe–Mg exchange potential has been recently suggested to control the formation of magnetite during serpentinization (Evans, 2008), this mechanism is unlikely in our natural systems. Because the chemical potential of iron is similar between the magnetite-bearing and -free serpentine-filled veins, and the variations of Fe value are probably results of the stable serpentine phase in the Mineoka serpentinites. These lines of evidences suggest that low silica activity is likely to facilitate the reaction of ferroan serpentine to form magnetite. One consequence of magnetite formation is the imposition of extremely reducing conditions on the system, and in turn, this resulted in the formation of iron alloys in the magnetite-bearing domains. Assemblages of sulfide and native-metal minerals in the Mineoka serpentinites also indicate low f_{O2} and f_{S2} during serpentinization (Sato and Ogawa, 2000).

The other key point is the absence of magnetite in the bastites (orthopyroxene pseudomorphs). The serpentine veins cutting the orthopyroxene have higher tetrahedral cations than those cutting serpentinized olivine, and they contain a mixture of serpentine and talc (Fig. 3B), which contrasts with the brucite–serpentine mixture in veins cutting olivine. The hydration of orthopyroxene is probably represented by the reaction:

$$6(Mg,Fe)SiO_3 + 3H_2O = (Mg,Fe)_3Si_2O_5(OH)_4 + (Mg,Fe)_3Si_4O_{10}(OH)_2$$

$$\text{orthopyroxene} + \text{water} = \text{serpentine} + \text{talc}. \quad (5)$$

The talc then releases silica into the hydrothermal fluid by the following reaction:

$$(Mg, Fe)_3Si_4O_{10}(OH)_2 + H_2O = (Mg, Fe)_3Si_2O_5(OH)_4 + SiO_2$$

$$\text{talc} + \text{water} = \text{serpentine} + \text{silica}. \quad (6)$$

The production of serpentine and talc is a result of an approximately two orders of magnitude higher silica activity than that needed for the production of the assemblages serpentine and brucite after olivine (Fig. 6). Magnetite is absent from the serpentine and talc assemblages replacing orthopyroxene, whereas the Fe values are similar for pseudomorphs after both olivine and orthopyroxene (Fig. 5), indicating that a low silica activity is crucial for the formation of magnetite during serpentinization. During the hydration of harzburgite, where orthopyroxene and olivine coexist, silica tends to move from talc-bearing portions to brucite-bearing portions. Variations in silica activity during serpentinization of peridotite depend on the relative rates of the hydration of olivine and orthopyroxene, and on fluid flow in the rocks. The occurrence of talc after orthopyroxene in the Mineoka serpentinites provides evidence for preservation of a large gradient in silica activity as the result of limited fluid pathways in the rocks. In the case of external supply of silica, such a model implies that olivine may hydrate without forming magnetite.

4. H_2- and CH_4-bearing fluid inclusions

Fluid-like inclusions are found in the relict olivine crystals. The inclusions are randomly distributed, but do not occur in secondary microfractures. The inclusions are generally less than 20 μm in size, and mostly contain two-phase inclusions (Fig. 7). We prepared doubly polished sections for laser Raman analysis to avoid contamination from adhesive agents. Raman spectra of the inclusions were obtained using the 514.5 nm line of an Ar laser (RENISHAW inVia Reflex). The laser beam was focused to a spot size of approximately 1 μm, and the spectra were scanned from 200 to 4400 cm^{-1}. The micro-inclusions were characterized by a strong band at 3698 cm^{-1}, in addition to the host olivine bands at 822 and 854 cm^{-1} (Fig. 8A). The 3698 cm^{-1} band is typical of chrysotile (Rinaudo et al., 2003), which indicates the inclusions are composed mainly of serpentine precipitated at low temperatures. These inclusions contain weak but detectable bands of CH_4 at 2916 cm^{-1} and H_2 at 4156 cm^{-1} (Fig. 8B, D). Although these vapor phases have been mostly removed from the matrix assemblages, the inclusions provide direct evidence of methane and hydrogen in the fluids during serpentinization. Phase equilibria indicates that the CH_4–H_2 bearing fluids were trapped under equilibrium conditions at temperatures below 300 °C, where lizardite and chrysotile are stable (Evans, 2004), and under markedly reducing

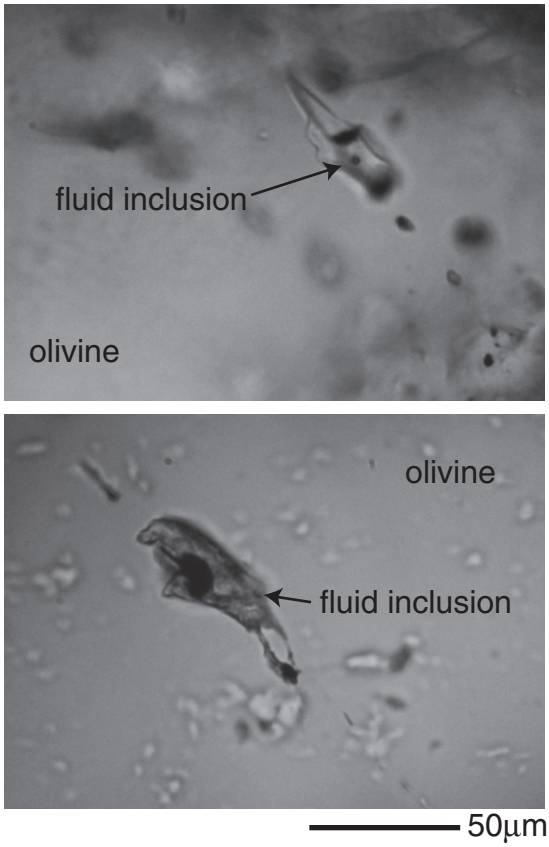

Fig. 7. Photomicrographs of fluid inclusions in olivine crystals (plane-polarized light), which are mostly filled with serpentine.

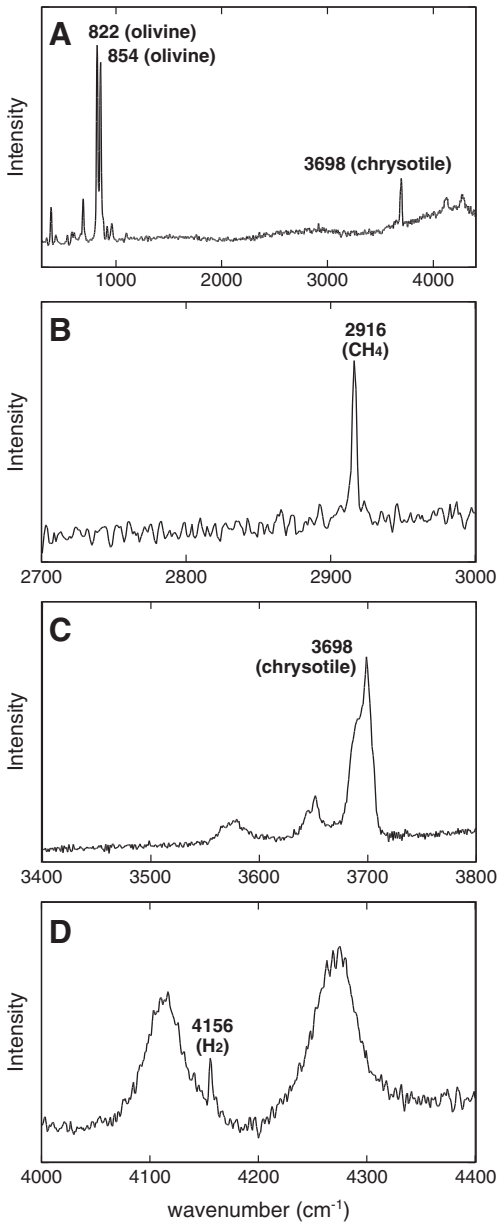

Fig. 8. Raman spectra of fluid inclusions in olivine. The spectrum as a whole (A) shows a band characterized by chrysotile at 3698 cm^{-1}, in addition to the host olivine bands at 822 and 854 cm^{-1}, suggesting that inclusions are mainly composed of low-temperature serpentine. Enlarged Raman spectra (B, D) show weak but detectable evidence for the vapor phases CH_4 (2916 cm^{-1}) and H_2 (4516 cm^{-1}) in the inclusions.

conditions. The absence of CO_2 as a fluid component suggests an extensive reduction of CO_2 to CH_4 in the H_2-rich hydrothermal vent systems. This is consistent with typical serpentine-hosted hydrothermal systems that exhibit high CH_4 concentrations along with an enrichment in H_2 (Donval et al., 1997; Charlou et al., 2002).

5. Implications and conclusions

The textural evolution of the Mineoka serpentinites shows that magnetite does not form directly from olivine. The magnetite-forming reaction involves a silica-out reaction, as witnessed by the lower abundance of serpentine in the magnetite-bearing veins, and the absence of magnetite in pseudomorphs after orthopyroxene. This suggests that the occurrence of magnetite is possible when there is a significant low silica activity in the fluids, implying that the system had locally evolved to lower silica activity during serpentinization. The magnetite formation results in the production of hydrogen and strongly reducing conditions, which may potentially support microbial activity in the vicinity of the seafloor (e.g., Kelley et al., 2001; Takai et al., 2004; McCollom, 2007). The CH_4 and H_2-bearing inclusions in relics of olivine provide direct evidence for the presence of CH_4 and H_2-rich hydrothermal vents during serpentinization, although those vapor phases have been almost entirely obliterated from the matrix assemblages. Our results indicate that, in addition to low oxygen fugacity, low silica activity is a key to generate hydrogen during serpentinization, and this is possible in rocks dominated by olivine, such as dunite, or locally, as a result of disequilibrium, in other silica-poor mantle rocks.

Acknowledgements

We thank Y. Takahashi, T. Naganuma and K. Michibayashi for comments and discussions. We also thank K. Okuzawa for help in the sample collection, Y. Shibata for microprobe analysis, and H. Hidaka and T. Hirotaka for laser Raman analysis. Constructive review by B. R. Frost and an anonymous reviewer are appreciated for improving the manuscript. This research was supported by the Japan Society for the Promotion of Science (JSPS).

References

Bach, W., Paulick, H., Garrido, C.J., Ildefonse, B., Meurer, W.P., Humphris, S.E., 2006. Unraveling the sequence of serpentinization reactions: petrography, mineral chemistry, and petrophysics of serpentinites from MAR 15°N (ODP Leg 209, Site1274). Geophys. Res. Lett. 33, L13306. doi:10.1029/2006GL025681.

Baronnet, A., Boudier, F., 2001. Microstructural and microchemical aspects of serpentinization. Lunar Planet. Sci. 3382 XI, Abst..

Baross, J.A., Hoffman, S.E., 1985. Submarine hydrothermal vents and associated gradient environments as sites for the origin and evolution of life. Orig. Life Evol. Biosph. 15, 327–345.

Beard, J., Frost, B.R., Fryer, P., McCaig, A., Searle, R., Ildefonse, B., Zinin, P., Sharma, S.K., 2009. Onset and progression of serpentinization and magnetite formation in olivine-richtroctolite from IODP Hole U1309D. J. Petrol. 50, 387–403.

Charlou, J.L., Donval, J.P., Fouquet, Y., Jean-Baptiste, P., Holm, N., 2002. Geochemistry of high H2 and CH4 vent fluids issuing from ultramafic rocks at the Rainbow hydrothermal field (36°14′N, MAR). Chem. Geol. 191, 345–359.

Corliss, J.B., Dymond, J., Gordon, L.I., Edmond, J.M., von Harzen, R.P., Ballard, R.D., Green, K., Williams, D., Bainbridge, A., van Crane, K., Andel, T.H., 1979. Submarine thermal springs on the Galapagos Rift. Science 203, 1073–1083.

Donval JP, Charlou JL, Donville E, Radford-Knoery J, Fouquet Y, Panzevera E, Jean-Baptiste P, Stievenard M, German C, FLORES Cruise Scientific Party, 1997. High H2 and CH4 content in hydrothermal fluids from Rainbowsite newly sampled at 36°14′ N on the AMAR segment Mid-Atlantic Ridge (diving FLORES cruise, July 1997): Comparison with other MAR sites. EOS Trans. AGU 78, FallMeet. Suppl., Abstract V51E-06.

Evans, B.W., 2004. The serpentinite multi-system revisited; chrysotile is metastable. Int. Geol. Rev. 46, 479–506.

Evans, B.W., 2008. Control of the products of serpentinization by the $Fe^{2+}Mg_{-1}$ exchange potential of olivine and orthopyroxene. J. Petrol. 49, 1873–7887.

Evans, B.W., Kuehner, S.M., Chopelas, A., 2009. Magnetite-free, yellow lizardite serpentinization of olivine websterite, Canyon Mountain complex, NE. Oregon. Am. Mineral. 94, 1731–1734.

Frost, B.R., Beard, J.S., 2007. On silica activity and serpentinization. J. Petrol. 48, 1351–1368.

Frost, B.R., Beard, J.S., 2008. On silica activity and serpentinization: Errata. J. Petrol. 49, 1253.

Hirauchi, K., Katayama, I., Uehara, S., Miyahara, M., Takai, Y., 2010. Inhabitation of subduction thrust earthquakes by low-temperature plastic flow in serpentine. Earth Planet. Sci. Lett. 295, 349–357.

Holm, N.G., Charlou, J.L., 2001. Initial indications of abiotic formation of hydrocarbons in the Rainbow ultramafic hydrothermal system, Mid-Atlantic Ridge. Earth Planet. Sci. Lett. 191, 1–8.

Kelley, D.S., Karson, J.A., Blackman, D.K., Früh-Green, G.L., Butterfield, D.A., Lilley, M.D., Olson, E.J., Schrenk, M.O., Roe, K.K., Lebon, G.T., Rivizzigno, P., the AT3-60 Shipboard Party, 2001. An off-axis hydrothermal vent field near the Mid-Atlantic Ridge at 30°N. Nature 412, 145–149.

Kelley, D.S., Karson, J.A., Früh-Green, G.L., Yoerger, D.R., Shank, T.M., Butterfield, D.A., Hayes, J.M., Schrenk, M.O., Olson, E.J., Proskurowski, G., Jakuba, M., Bradley, A., Larson, B., Ludwig, K., Glickson, D., Buckman, K., Bradley, A.S., Brazelton, W.J., Roe, K., Elend, M.J., Delacour, A., Bernasconi, S.M., Lilley, M.D., Baross, J.A., Summons, R.E., Sylva, S.P., 2005. A serpentinite-hosted ecosystem: the Lost City hydrothermal field. Science 307, 1428–1434.

Martin, W., Baross, J., Kelley, D.S., Russell, M.J., 2008. Hydrothermal vents and the origin of life. Nat. Rev. Microbiol. 6, 805–814.

McCollom, T.M., 2007. Geochemical constraints on sources of metabolic energy for chemolithoautotrophy in ultramafic-hosted deep-sea hydrothermal systems. Astrobiology 7, 933–950.

Nakamura, K., Morishita, T., Bach, W., Klein, F., Hara, K., Okino, K., Takai, K., Kumagai, H., 2009. Serpentinized troctolites exposed near the Kairei Hydrothermal Field. Central Indian Ridge: insights into the origin of the Kairei hydrothermal fluid supporting a unique microbial ecosystem. Earth Planet. Sci. Lett. 208, 128–136.

Ogawa, Y., Taniguchi, H., 1988. Geology and tectonics of the Miura–Boso Peninsulas and adjacent area. Mod. Geol. 12, 147–168.

Oufi, O., Cannat, M., Horen, H., 2002. Magnetic properties of variably serpentinized abyssal peridotite. J. Geophys. Res. 107. doi:10.1029/2001JB000549.

Rinaudo, C., Gastaldi, D., Belluso, E., 2003. Characterization of chrysotile, antigorite and lizardite by FT-Raman spectroscopy. Can. Mineral. 41, 883–890.

Sato, H., Ogawa, Y., 2000. Sulfide minerals as an indicator for petrogenesis and serpentinization of peridotites: an example from Hayama–Mineoka belt, central Japan. In: Dilek, Y., Moores, E., Elton, D., Nicolas, A. (Eds.), Ophiolites and Oceanic Crust: New Insights from Field Studies and Ocean Drilling Program: Geological Society of America, vol. 349, pp. 427–437.

Sato, H., Taniguchi, H., Takahashi, N., Mohiuddin, M.M., Hirano, N., Ogawa, Y., 1999. The origin of the Mineoka ophiolite. J. Grograph., Tokyo Geograph. 108, 177–189 (Japanese with English abstract).

Sleep, N.H., Meibom, A., Fridriksson, T., Coleman, R.G., Bird, D.K., 2004. H_2-rich fluids from serpentinization: geochemical and biotic implications. Proc. Natl Acad. Sci. USA 101, 12818–12823.

Spiess, F.N., Macdonald, K.C., Atwater, T., Ballard, R., Carranza, A., Cordoba, D., Cox, C., Daiz Garcia, V.M., Francheteau, J., Guerrero, J., Hawkins, J., Haymon, R., Hessler, R., Juteau, T., Kastner, M., Larson, R., Luyendyk, B., Macdougall, J.D., Miller, S., Normark, W., Orcutt, J., Rangin, C., 1980. East Pacific Rise: hot springs and geophysical experiments. Science 207, 1421–1433.

Takai, K., Gamo, T., Tsunogai, U., Nakayama, N., Hirayama, H., Nealson, K.H., Horikoshi, K., 2004. Geochemical and microbiological evidence for a hydrogen-based, hyperthermophilic subsurface lithoautotrophic microbial ecosystem (HyperSLiME) beneath an active deep-sea hydrothermal field. Extremophiles 8, 269–282.

Toft, P.B., Arkani-Hamed, J., Haggerty, S.E., 1990. The effects of serpentinization on density and magnetic susceptibility: a petrophysical model. Phys. Earth Planet. Int. 65, 137–157.

Wicks, F.J., Whittaker, E.J.W., 1977. Serpentine texture and serpentinization. Can. Mineral. 13, 227–243.